


Preaggregation of Asphaltenes in the Presence of Natural Polymers by Molecular Dynamics Simulation

Lucas G. Celia-Silva, Patrícia B. Vilela, Pedro Morgado, Elizabete F. Lucas, Luís F. G. Martins,* and Eduardo J. M. Filipe*

 Cite This: *Energy Fuels* 2020, 34, 1581–1591

 Read Online

ACCESS |

 Metrics & More

 Article Recommendations

ABSTRACT: Cashew nut shell liquid (CNSL), its extract, cardanol, and polycardanol, are known to influence the dispersion behavior of asphaltenes in model solvent mixtures. CNSL and cardanol act as dispersants, while polycardanol can act as both dispersant or flocculant depending on its molecular architecture, concentration, and asphaltene source. In this work, the preaggregation of asphaltenes in model solvents (toluene, *n*-heptane, and their mixtures) has been studied by atomistic molecular dynamics simulation. The influence of cardanol, addition polycardanol, and condensation polycardanol as additives has been addressed. The simulation results remarkably reproduce the experimental trends, thus contributing to a better understanding of the molecular processes underlying the stabilization or precipitation of asphaltenes by cardanols and their polymers.

1. INTRODUCTION

Asphaltenes are often considered the heaviest and the most polar fraction of crude oil¹ and are particularly abundant in heavy oils, which have been increasingly used as raw materials in the last few decades.² Being a complex mixture of thousands of compounds,^{3,4} their definition is rather practical in nature: asphaltenes are the fraction of crude oil that is insoluble in *n*-alkanes, such as *n*-pentane and *n*-heptane, and soluble in aromatic solvents, such as benzene and toluene.^{5,6} This behavior is often the basis of asphaltene stability studies.

Two main models have been proposed to describe the molecular structure of typical components of asphaltene fractions.⁷ The island (or continental) model^{8,9} considers the asphaltene molecule as a unique large core of condensed aromatic rings with aliphatic side chains; the archipelago model^{10,11} describes the asphaltene molecule as containing two or more small aromatic cores connected by aliphatic chains. In both models, heteroatoms (N, S, and O) are present both in the aromatic rings and in the aliphatic chains, as well as metals, such as Vanadium and Nickel. Although the archipelago model has been able to describe some details of asphaltenes' behavior in solution,¹² the island model is the most widely accepted.¹³ Asphaltenes display, on average, between 4 and 10 aromatic rings in their core, lateral aliphatic chains with 6–7 carbon atoms, and molecular weights between 400 and 1000 g mol⁻¹.¹⁴

According to the Yen–Mullins model,^{15–17} asphaltenes tend to assemble in aliphatic media forming nanoaggregates with less than 10 molecules, which in turn are able to form larger structures (clusters) with diameters of about 5 nm.¹⁸ It is thought that the main driving force of aggregation is the π – π stacking or aromatic interactions between the aromatic cores, while the steric hindrance caused by aliphatic side chains tends to limit aggregation.¹⁹ Three different spatial configurations

have been proposed: face-to-face or parallel, offset stacking or offset parallel, and edge-to-face or T-shape.¹⁶ Naturally stabilized in oil, asphaltene molecules tend to flocculate and precipitate as a consequence of subtle changes in composition, temperature, or pressure during oil extraction or processing. Asphaltenes adsorb to the internal pipeline surfaces changing their wettability and tend to stabilize water-in-oil emulsions,²⁰ making the separation of oil from naturally occurring water-in-oil wells more difficult. Asphaltene deposits formed in this process cause clogging of pipelines and wellbores, reducing oil flow and production rate, with high economic and environmental costs.¹

The problem has been addressed using chemical additives to prevent or minimize the precipitation of asphaltenes in oil. According to early studies, asphaltene dispersions in oil are stabilized by naturally occurring resins. These are perceived as amphiphilic molecules containing aromatic and aliphatic moieties²¹ that are able to “peptize” asphaltenes,^{22,23} preventing their stacking and subsequent precipitation. Recent simulation and experimental studies,^{12,24,25} however, were not able to identify significantly strong interactions between molecular models of asphaltenes and resins. In general, amphiphilic additives have been chosen to try to mimic natural systems. Alkylphenols, alkylbenzene sulfonic acids, fatty acids, amino alcohols, ionic liquids (ILs), and surface-active polymers are among the most tested substances. They are expected to interact significantly with the asphaltene molecules, which are considered to be weak electron donors

Received: October 24, 2019

Revised: December 19, 2019

Published: January 9, 2020

and strong hydrogen bond (HB) acceptors,^{26–28} due to the presence of heteroatoms. Chang and Fogler^{29,30} experimentally studied the asphaltene stabilization potential of alkylbenzene-derived amphiphiles, such as alkylphenols and alkylbenzene sulfonic acids, concluding that stabilization is enhanced by increasing the polarity, hydrogen-bonding capacity, and mainly the acidity of the amphiphile's head group. The efficiency of the additive also increases with the chain length, and a minimum length seems to be necessary to create a hydrophobic steric stabilization layer that decreases the tendency to aggregate. More recent studies^{31,32} confirmed that the addition of alkylphenols and alkylbenzene sulfonic acids decreases the average dimension of asphaltene clusters in toluene/*n*-heptane solvent mixtures.

Ionic liquids (IL) are another important class of substances that have been tested as additives for asphaltene stabilization. Hu and Guo³³ studied the stabilizing potential of pyridinium and isoquinolinium-based IL with different side-chain lengths and anions in CO₂-injected oil samples at high pressures. It is important to note that the presence of carbon dioxide in the system promotes asphaltene aggregation and flocculation,³⁴ and finding an effective stabilizing agent for these conditions is a more difficult task.

Asphaltene aggregation has been extensively studied by computer simulation. These studies confirmed the stacking of aromatic cores³⁵ forming dimers, trimers, and tetramers³⁶ and the existence of different orientations: face–face, offset stacked, and T-shaped. Pacheco-Sánchez et al.³⁷ also showed that aliphatic side chains tend to hinder asphaltene aggregation, while Carauta et al.³⁸ found that the asphaltene–asphaltene distance in aggregates is smaller in *n*-heptane than in toluene. Sedghi et al.¹⁹ reported that the asphaltene dimerization energy increases with the number of aromatic rings in the aromatic core, but remains almost constant with different sizes of the alkyl side chains. Studies of asphaltene aggregation in the presence of dispersing additives by computer simulation are scarce in the literature. Headen and Boek,³⁹ for example, used molecular simulations to study asphaltene aggregation in supercritical CO₂ using limonene as an additive and concluded that 50% (w/w) of limonene significantly reduces asphaltene aggregation. More recently, Headen et al.¹² studied asphaltene aggregation, with and without resins, in *n*-heptane and toluene, using both island and archipelago models.

The properties of asphaltenes and their behavior in oil have also been modeled by molecular-based equations of state, such as PC-SAFT.^{40,41} Good agreement was found between theoretical predictions and experimental results for phase equilibria and the *pVT* properties of oil rich in asphaltenes.

The Lucas research group has long been using polymers as additives with dispersing/flocculating action on asphaltene dispersions. They tested^{42,43} cashew nut shell liquid (CNSL), its fraction cardanol (a mixture of phenolic compounds containing 15-carbon aliphatic chains with variable unsaturation degrees, *meta*-substituted in an aromatic ring) and polycardanol (from the cardanol polymerization) as additives for asphaltene stabilization in model mixtures. A dispersion effect was found for CNSL and cardanol comparable to nonylphenol, and a flocculating effect was observed for addition polycardanol. According to the authors, the number and steric hindrance of hydroxyl groups prevent their interaction with the asphaltene heteroatoms, granting a significant polarity to the surface of the asphaltene-additive

nanoaggregates, which tend to precipitate in apolar solvents. The same group⁴⁴ used polycardanol obtained by two different synthetic routes (addition and condensation)⁴⁵ to perform asphaltene stability tests and assess the influence of additive molecular architecture. Their main conclusions were as follows: (1) addition polycardanol stabilizes asphaltenes more efficiently than condensation polycardanol, probably because the molecular structure of the former allows hydroxyl groups to be more accessible to interact with asphaltenes; (2) for both polymers, there is a concentration at which the stabilizing effect is maximum; (3) condensation polycardanol displays flocculating effects; (4) polycardanol stabilizes asphaltenes more efficiently than the cardanol monomer; (5) the stabilizing effect of the additives correlates with their demulsifying ability in water-in-oil emulsions; and (6) both the stabilizing effect and the demulsifying action depend on the molecular weight of the additive. More recently, poly(ionic liquids) obtained from cardanol⁴⁶ were found to stabilize asphaltenes and induce separation of water/oil emulsions.

In this work, we have studied asphaltene preaggregation phenomena in typical model solvents (*n*-heptane, toluene, and an *n*-heptane/toluene mixture) by atomistic molecular dynamics simulation. Additionally, the influence of three additives in preaggregation has been addressed: cardanol, addition polycardanol, and condensation polycardanol. The simulation results remarkably reproduce the experimental trends obtained by Lucas et al., thus contributing to a better understanding of the molecular processes underlying the stabilization or precipitation of asphaltenes in relevant media by cardanols and their polymers.

2. SIMULATION DETAILS

Molecular dynamics simulations of asphaltenes in *n*-heptane, toluene, and an *n*-heptane/toluene mixture have been carried out with and without dispersing/precipitating agents, such as cardanol and polycardanol obtained by addition and condensation. The interaction between asphaltene and additives as well as preaggregation events, have been studied based on the structural and dynamic properties of the systems obtained from the analysis of simulation trajectory output files.

2.1. Models. An atomistic approach was employed in this work, being the optimized potentials for liquid simulations all-atom (OPLS-AA) force-field⁴⁷ framework used to model all of the studied compounds. This force-field models each atom as an interaction site, and the potential energy is written as the sum of contributions due to bond stretching, bond angle bending, dihedral angle torsion, improper dihedral angles, and nonbonded interactions (van der Waals plus electrostatic interactions). For both solvents (toluene and *n*-heptane), the parameters from the OPLS-AA original papers were used, except for the atomic partial charges of toluene, for which the reparameterization by Udier-Blagović et al.⁴⁸ was employed. The validation of the chosen parameters was done by determining pure liquid densities and self-diffusion coefficients of each solvent at one temperature, and the results are presented in Table 1. The agreement between simulated and experimental density is excellent for *n*-heptane. For toluene, a deviation of 2.3% is well within the generally accepted range for this property, which is 4%. As for the diffusion coefficients, it is well known that the simulation of transport properties is a very challenging task. Large deviations are frequent, even for simple fluids using force fields that accurately reproduce the

Table 1. Comparison between Simulated and Experimental Results of Density and Self-diffusion Coefficient for Toluene and *n*-Heptane at 298.15 K

	ρ (sim.) (kg m ⁻³)	ρ (exp.) (kg m ⁻³)	D (sim.) (m ² s ⁻¹)	D (exp.) (m ² s ⁻¹)
toluene	882.0	862.3 ⁵¹	1.03×10^{-9}	2.18×10^{-9} ⁵²
<i>n</i> -heptane	671.1	679.9 ⁵³	2.38×10^{-9}	3.12×10^{-9} ⁵⁴

equilibrium properties. The predicted diffusion coefficients can thus be considered to be quite good.

A single molecular structure was chosen to model asphaltene (Figure 1). The molecule was designed in such a way that its

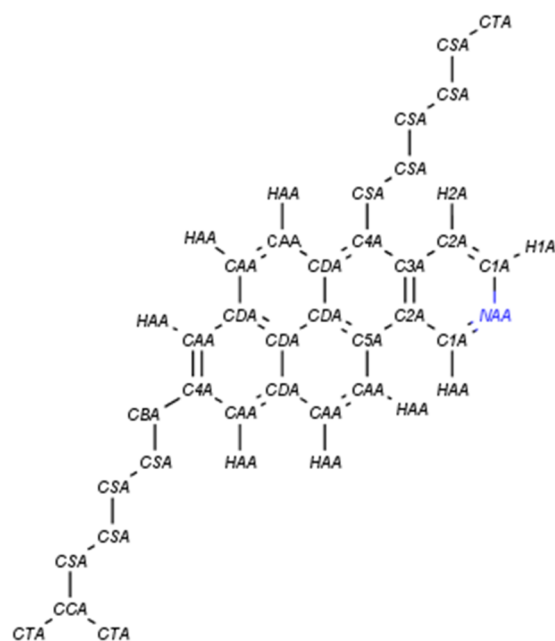


Figure 1. Molecular structure of the asphaltene model used in this work (atoms whose code name begins with: C, carbon; H, hydrogen; and N, nitrogen).

main molecular characteristics match those experimentally obtained for a real asphaltene subfraction by Ferreira et al.⁴⁹ A comparison between experimental and model properties is shown in Table 2. A model for the pyridine ring from Coleman

Table 2. Comparison of Some Key Properties between the Chosen Asphaltene Model for Simulations and One of the Experimentally Obtained Subfractions by Ferreira et al.⁴⁹: Molecular Weight, Aliphatic and Aromatic Hydrogen Percent and Nitrogen Percent

	model	experimental
M_m (g mol ⁻¹)	449.7	445
% $H_{\text{aliphatic}}$	77	78
% H_{aromatic}	23	22
% N	3.11	1.14

et al.⁵⁰ was used as a starting point, the partial charges of the atoms from alkyl side chains were chosen according to the OPLS-AA model for alkanes⁴⁷ and those of the atoms from internal aromatic rings were adjusted to keep the whole molecule neutral.

Cardanol was considered as a meta-substituted phenol, with an alkyl side chain comprising 15 carbon atoms and containing

a single unsaturation between carbons 8 and 9 (Figure 2). It was modeled using a phenol ring as a starting point following the reparameterization by Coleman et al.⁵⁰ The partial charge of the first carbon atom of the aliphatic chain was also adjusted to keep the molecule neutral. Simple models of polycardanol were used, taking into account the two main polymerization methods of cardanol (Figures 3 and 4). For polycardanol obtained by addition (monomers connected by double bond opening), a trimer was considered, for which steric hindrance is already apparent. In the case of polycardanol obtained by condensation (connection by the aromatic ring, usually experimentally obtained using formaldehyde as the polymerization agent), a heptamer was considered.

Following the OPLS-AA parameterization, geometrical combining rules were used to compute the nonbonded Lennard-Jones interactions between sites of different types

$$\epsilon_{ij} = \sqrt{\epsilon_i \epsilon_j} \quad (1)$$

$$\sigma_{ij} = \sqrt{\sigma_i \sigma_j} \quad (2)$$

For nonbonded interactions between sites in the same molecule, only sites separated by three or more bonds are considered. Nonbonded interactions between sites separated by three bonds are scaled by a factor of 0.5. In this work, all bonds involving hydrogen were treated as rigid, with the respective length fixed at the equilibrium distance using the SHAKE algorithm.⁵⁵

2.2. Methods. Molecular dynamics simulations were performed using both *DL_POLY Classic*⁵⁶ and GROMACS 5.1.5^{57,58} packages, in cubic boxes containing approximately between 300 and 500 molecules, with periodic boundary conditions in all three directions. The initial liquid box sizes were established according to the experimental densities. For each system, the following simulation protocol was applied: an initial short simulation for system relaxation, followed by a *NpT* equilibration run of 3 ns and a 50 ns long *NVT* production run, which was used to obtain the structural and dynamic properties of the system. These simulations were performed at 298.15 K and, for equilibration, 1 atm. The equations of motion were solved using the leapfrog integration algorithm, with a time step of 2 fs. All of the systems were coupled to the Nosé–Hoover thermostat^{59,60} with a coupling constant of 0.5 ps and, for simulations in *NpT* ensembles, also coupled to the Nosé–Hoover or Parrinello–Rahman barostat with a coupling constant of 0.2 ps. An initial velocity obtained from a Maxwell distribution at the desired initial temperature has been assigned to all atoms.

Both nonbonded Lennard-Jones and electrostatic potential were truncated using cut-offs of 12 Å, and analytical tail corrections to dispersion terms were added. The long-range electrostatic (Coulombic) interactions beyond the cutoff were calculated using the Ewald sum method.⁶¹ The obtained trajectories were visualized using the Visual Molecular Dynamics⁶² program; the nanoaggregation analysis and radial distribution function calculations were performed using the TRAVIS software.⁶³ In the simulation protocol, the attainment of the equilibrium is confirmed by the analysis of the variations of all of the energy components of the systems. A maximum energy variation of 0.4% is considered for equilibrium testing. The conformational energy of the different molecules was obtained from the simulation trajectories and confirmed to remain constant within the simulation time, an indication that very probably conformational equilibrium has been reached.

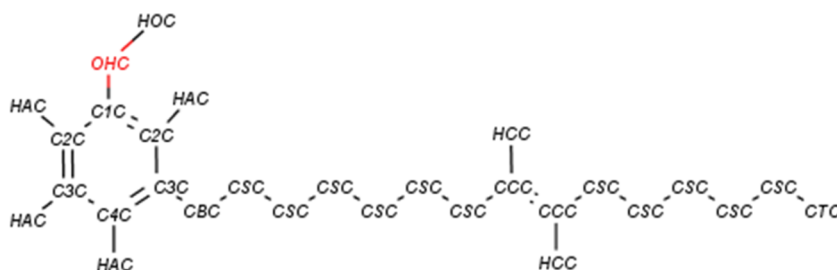


Figure 2. Molecular structure of the cardanol model used in this work (atoms whose code name begins with: C, carbon; H, hydrogen; and O, oxygen).

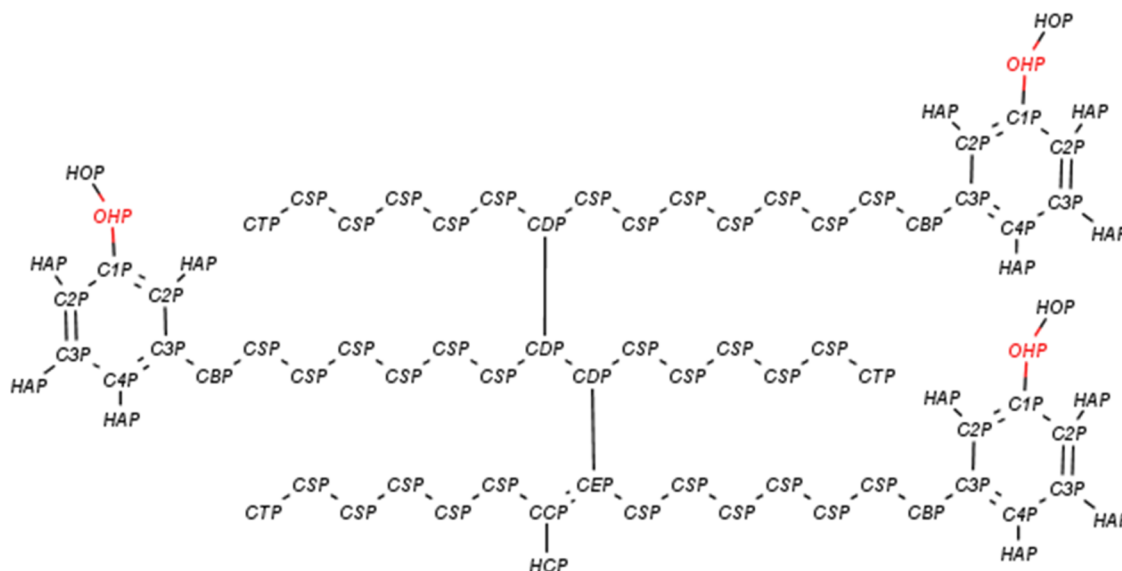


Figure 3. Molecular structure of the polycardanol model obtained by addition used in this work (atoms whose code name begins with: C, carbon; H, hydrogen; and O, oxygen).

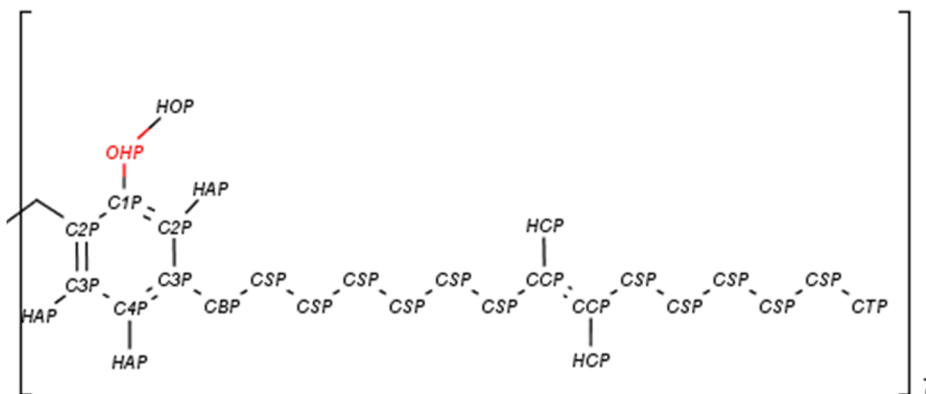


Figure 4. Molecular structure of the polycardanol model obtained by condensation used in this work (atoms whose code name begins with: C, carbon; H, hydrogen; and O, oxygen).

2.3. Systems. The asphaltene/additive preaggregation studies by simulation were carried out in toluene/*n*-heptane solvent mixtures with the same volumetric proportion: 70:30 (v/v) for all of the systems. For comparison purposes, pure toluene or pure *n*-heptane were also used as solvents in some cases. The systems studied are listed in Table 3.

3. RESULTS AND DISCUSSION

3.1. Asphaltene Aggregation in Toluene, *n*-Heptane, and Their Mixtures.

Before addressing the aggregation

process itself, an attempt was made to characterize the molecular interactions between the asphaltene molecules and the studied solvents in terms of the structure/composition of the asphaltene solvation sphere. This was probed simulating a single asphaltene molecule in a box containing a 2:1 molar (70/30 volumetric) toluene/*n*-heptane mixture. In Figure 5, the radial distribution functions (rdf), $g(r)$, between two asphaltene carbons (an aromatic and an aliphatic) and terminal aliphatic carbon atoms of each solvent are presented.

Table 3. Number of Molecules of Each Compound and Mass Fractions of Asphaltene and Additive for Each Mixture Studied

system	number of molecules	mass composition (%)
1A200T100H	asphaltene: 1 toluene: 200 <i>n</i> -heptane: 100	asphaltene: 1.6
10A200T100H	asphaltene: 10 toluene: 200 <i>n</i> -heptane: 100	asphaltene: 13.6
10A300T	asphaltene: 10 toluene: 300	asphaltene: 14
10A300H	asphaltene: 10 <i>n</i> -heptane: 300	asphaltene: 13
10A300T20C	asphaltene: 10 cardanol: 20 toluene: 300	asphaltene: 11.8 cardanol: 15.8
10A200T100H20C	asphaltene: 10 cardanol: 20 toluene: 200 <i>n</i> -heptane: 100	asphaltene: 11.5 cardanol: 15.5
10A300H20C	asphaltene: 10 cardanol: 20 <i>n</i> -heptane: 300	asphaltene: 11.1 cardanol: 14.9
10A300T6PCA	asphaltene: 10 addition polycardanol: 6 toluene: 300	asphaltene: 12 addition polycardanol: 14.5
10A200T100H6PCA	asphaltene: 10 addition polycardanol: 6 toluene: 200 <i>n</i> -heptane: 100	asphaltene: 11.7 addition polycardanol: 14.2
10A300H6PCA	asphaltene: 10 addition polycardanol: 6 <i>n</i> -heptane: 300	asphaltene: 11.2 addition polycardanol: 13.6
10A300T3PCC	asphaltene: 10 condensation polycardanol: 3 toluene: 300	asphaltene: 11.6 condensation polycardanol: 17.1
10A200T100H3PCC	asphaltene: 10 condensation polycardanol: 3 toluene: 200 <i>n</i> -heptane: 100	asphaltene: 11.4 condensation polycardanol: 16.7
10A300T3PCC	asphaltene: 10 condensation polycardanol: 3 <i>n</i> -heptane: 300	asphaltene: 10.9 condensation polycardanol: 16.1

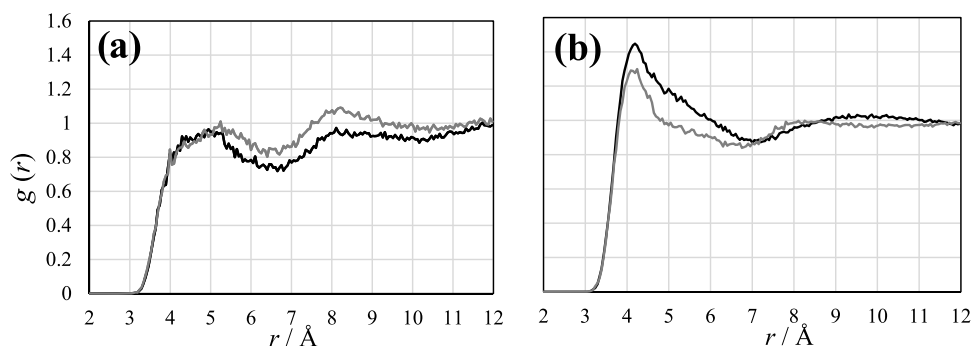


Figure 5. Radial distribution functions of the terminal aliphatic carbon atom from *n*-heptane (black curves) and toluene (gray curves) around asphaltene atoms. (a) Aromatic carbon atom (C5A) and (b) terminal aliphatic carbon atom.

As can be seen, the asphaltene aromatic carbon atoms are preferably surrounded by toluene, whereas the aliphatic carbon atoms by *n*-heptane. These results are in agreement with the experimental evidence of π - π interaction between the

asphaltene aromatic core and the toluene aromatic ring and also the affinity between the asphaltene alkyl side chains and aliphatic solvents. It is also interesting to note that the $g(r)$ involving asphaltene aromatic carbon atoms presents values

smaller than unity in almost the entire distance range studied, which is an indication of a relatively hindered interaction between asphaltene and each solvent. This effect can also be observed in Figure 6, where spatial distribution functions

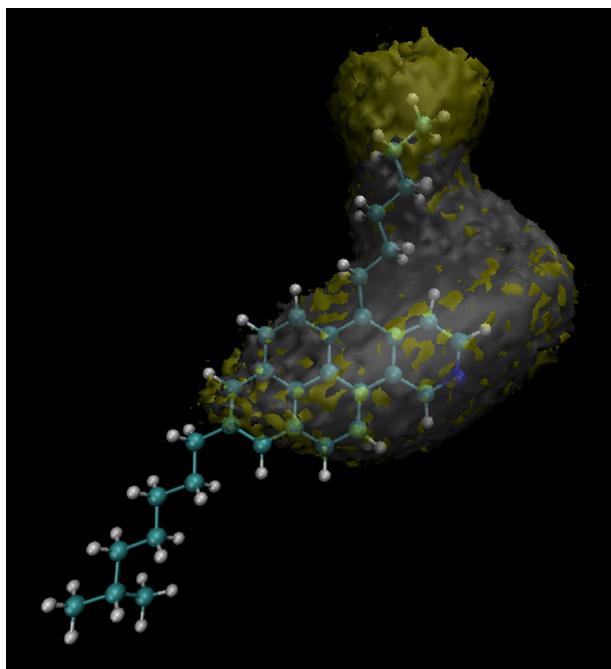


Figure 6. Spatial distribution functions of *n*-heptane (terminal carbon atom, yellow) and toluene (*meta*-carbon atom, silver) around asphaltene showing the isodensity surfaces with isovalues of 0.01 nm^{-3} for *n*-heptane and 0.04 nm^{-3} for toluene.

between asphaltene molecules and specific atoms of *n*-heptane and toluene in the solvent mixture studied are shown. As can be seen, *n*-heptane shows a clear preference to surround the asphaltene hexyl chain.

The asphaltene preaggregation in each solvent was studied simulating 10 asphaltene molecules in pure toluene, pure *n*-heptane, and the same 2:1 mixture of toluene/*n*-heptane. The process of dimerization of the asphaltene molecules was first checked. The detection of dimers during the simulation was subjected to an asphaltene–asphaltene distance criterion as used by Goual et al.³¹ taking a central aromatic carbon from the asphaltene molecule, a dimer is considered to form when the distance between any pair of such atoms of different asphaltene molecules becomes less than 8.5 \AA and deform when this distance exceeds 10 \AA . Using this criterion, asphaltene dimerization events were counted in pure toluene, pure *n*-heptane, and their mixture. The results are presented in Figure 7 as a function of the dimer lifetime. As expected, asphaltene dimers of almost all lifetimes are much more frequent in *n*-heptane than in toluene, in agreement with the different solubility of asphaltenes in each solvent. The dimer frequency shows intermediate values for the toluene/*n*-heptane mixture, although closer to that of pure *n*-heptane, which can be an indication that the *n*-heptane fraction used (0.33 mole fraction) is enough to perturb the asphaltene dispersion. In fact, a volume fraction of 30% in *n*-heptane is frequently reported in the literature as the stability limit for asphaltene dispersions in this kind of model systems.³¹

Aggregates larger than dimers were also evaluated, and the aggregation number distribution of asphaltene molecules in

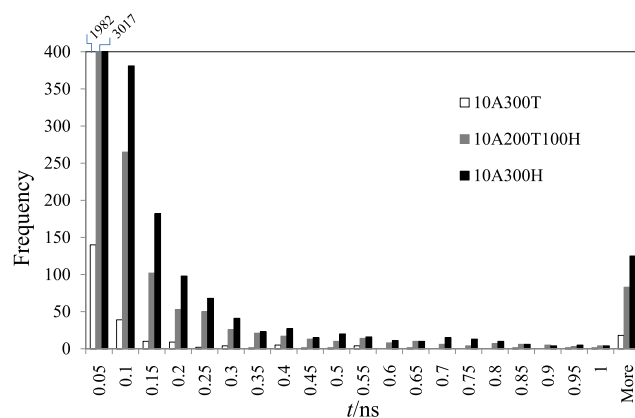


Figure 7. Frequency of asphaltene dimer formation as a function of its lifetime in toluene (white bars), *n*-heptane (black bars), and a 2:1 molar toluene/*n*-heptane binary mixture (gray bars), for a 50 ns production simulation (simulation box contained 10 asphaltene molecules and 300 solvent molecules).

each solvent was calculated. As before, a distance criterion was used: starting with a dimer, larger aggregates were counted whenever the central atom of a third, fourth, ... asphaltene molecule approaches within 8.5 \AA . The calculations were performed using the program of Bernardes et al.^{64,65} The occurrence probability of asphaltene aggregates for each size (in the number of molecules) is represented as a histogram in Figure 8. As can be seen, while monomers are more frequent in

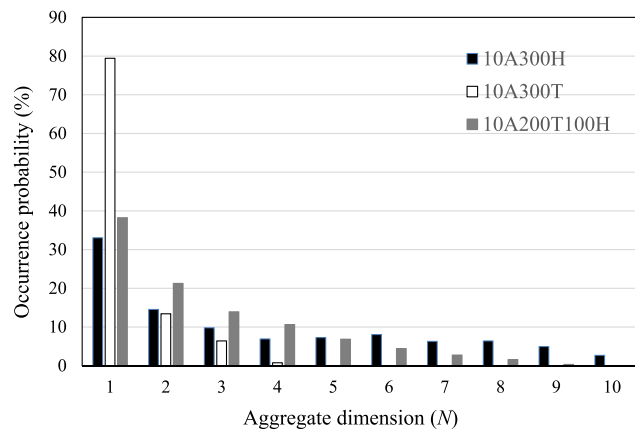


Figure 8. Occurrence probability of asphaltene aggregates as a function of aggregate size (number of asphaltene molecules) in toluene (white bars), *n*-heptane (black bars), and the binary mixture toluene/*n*-heptane (2:1 molar, gray bars). Boxes with 10 asphaltene molecules and 300 solvent molecules.

toluene, larger clusters are, in general, more frequent in *n*-heptane. In particular, clusters of 6 or more asphaltene molecules (out of a total of ten) are almost absent in toluene but quite frequent in *n*-heptane. The model predicts the formation of larger asphaltene clusters in *n*-heptane than in toluene. Again, the behavior in the binary mixture is intermediate between that observed in the pure solvents, although much closer to pure *n*-heptane. It is important to stress that molecules located within 8.5 \AA from each other are considered to belong to the same aggregate. The “stronger” interaction between asphaltene molecules in *n*-heptane is further proved by the inspection of radial distribution functions between central atoms (CSA) of asphaltene molecules (Figure

9) in each pure solvent and their binary mixture. As can be seen, the $g(r)$ obtained in *n*-heptane is much more intense than

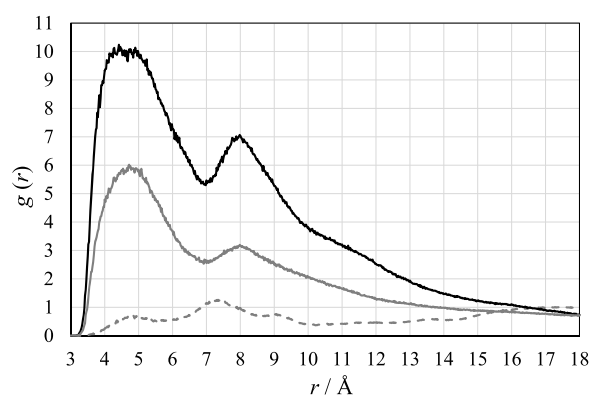


Figure 9. Radial distribution functions ($g(r)$) between internal aromatic carbon atoms of asphaltenes (CSA) in toluene (dashed gray), *n*-heptane (black), and in 2:1 molar toluene/*n*-heptane mixture (gray).

that obtained in toluene. Again, in the binary mixture, the results are intermediate between those of the pure solvents, although closer to *n*-heptane. All of the $g(r)$ present two major peaks at distances of approximately 4–5 Å and 7–8 Å, which suggests two different orientations of asphaltene molecules around each other, a parallel one and a perpendicular one. The figure shows that the most probable configuration of asphaltene molecules in *n*-heptane and in the mixture corresponds to the smaller distance (4.4 and 4.7 Å, respectively), and in toluene, it corresponds to the largest distance (7.3 Å). It can also be seen that the first peak appears at a shorter distance in *n*-heptane (4.4 Å) than in the mixture (4.7 Å) and that at a shorter distance than in toluene (4.8 Å). However, the second peak is located at a shorter distance in toluene (7.3 Å) than in *n*-heptane or in the mixture (8 Å). These observations seem to indicate that: (1) asphaltene molecules are on average nearer to each other in *n*-heptane than in toluene; (2) in *n*-heptane, asphaltene molecules prefer the parallel orientation, while the perpendicular orientation seems to be preferred in toluene.

3.2. Influence of Additives on Asphaltene Preaggregation in Toluene, *n*-Heptane, and Their Mixtures.

The influence of additives on asphaltene aggregation was studied using a simulation box containing 10 asphaltene molecules and 20 cardanol molecules, or 6 addition polycardanol or 3 condensation polycardanol in pure toluene, *n*-heptane, and in a toluene/*n*-heptane mixture. The lifetime distribution of the asphaltene dimers in the absence and presence of each additive in each solvent is shown in Figure 10. As can be seen, cardanol seems to reduce the formation of asphaltene dimers of almost all lifetimes acting as a dispersing agent. The effect of polycardanols depends on the nature of the solvent. They clearly reduce the number of asphaltene dimers of all lifetimes in *n*-heptane and in the *n*-heptane/toluene mixture. In toluene, however, the additives seem to promote the formation of dimers. The competition between asphaltene and additives by the solvent molecules can be viewed as the reason for this phenomenon. For almost the same number of aromatic rings in the systems involving each additive, the enhanced steric hindrance presented by the polymeric additives may require more solvent molecules to adequately

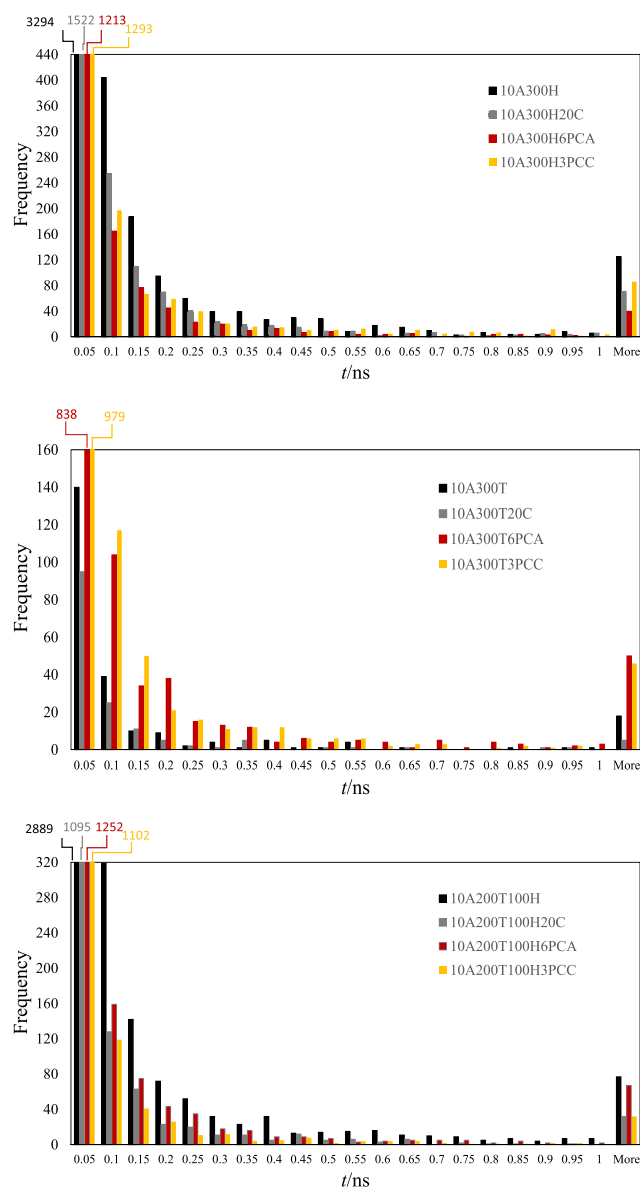


Figure 10. Histogram showing the frequency of asphaltene dimer formation as a function of its duration in (a) *n*-heptane, (b) *n*-heptane/toluene and (c) toluene, for a 50 ns production simulation in the absence of additive (black); with cardanol (gray) with polycardanol by addition (dark red) and with polycardanol by condensation (yellow). Boxes containing 10 asphaltene molecules, 300 *n*-heptane molecules, and 20 cardanol molecules or 6 addition polycardanol molecules or 3 condensation polycardanol molecules.

solvate them, which may lead to a solvent depletion around asphaltene units and promote their dimerization. Polycardanols seem to be more efficient as aggregation preventing agents than cardanol in *n*-heptane, less efficient in toluene, and comparable to it in the solvent mixture. On the other hand, addition polycardanol is more efficient than condensation polycardanol in *n*-heptane and less efficient in *n*-hexane/toluene.

The occurrence probability of asphaltene aggregates larger than dimers was also calculated in all solvents, with and without additives. It is shown in Figure 11 as a function of aggregate size. In *n*-heptane, condensation polycardanol seems to promote the formation of asphaltene clusters containing between 3 and 5 molecules and prevent the formation of larger

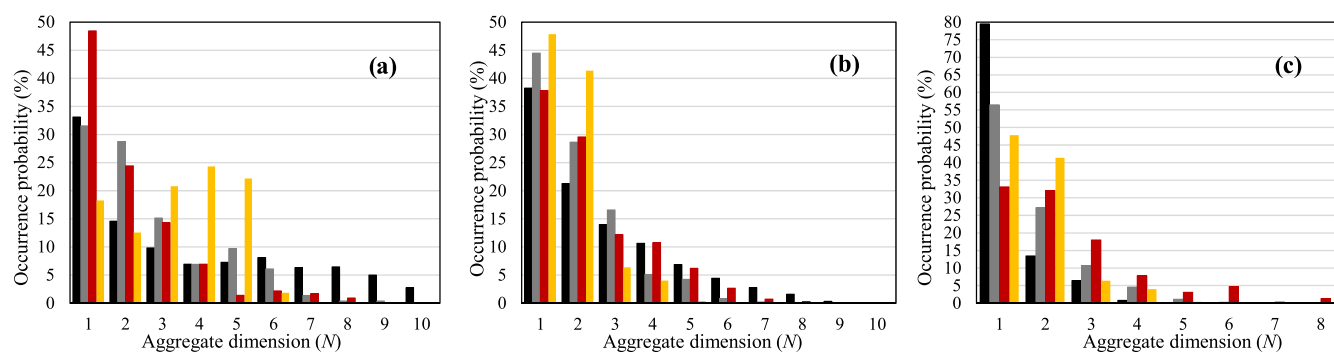


Figure 11. Occurrence probability of asphaltene aggregates as a function of aggregate dimension (number of asphaltene molecules) in *n*-heptane (a), a toluene/*n*-heptane mixture, (b) and toluene (c) for a 50 ns production simulation in the absence of additive (black); with cardanol (gray); with polycardanol by addition (dark red) and with polycardanol by condensation (yellow). Boxes containing 10 asphaltene molecules, 300 solvent molecules (200 toluene molecules and 100 *n*-heptane molecules in the case of b), and 10 cardanol molecules or 6 addition polycardanol molecules or 3 condensation polycardanol molecules.

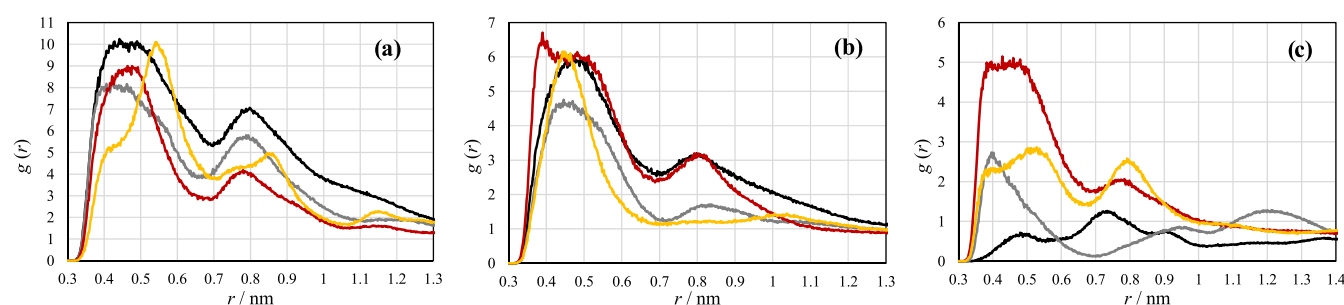


Figure 12. Radial distribution functions ($g(r)$) between aromatic CSA asphaltene atoms in *n*-heptane (a), a toluene/*n*-heptane mixture (b), and toluene (c) with no additive (black); with cardanol (gray); with addition polycardanol (dark red) and with condensation polycardanol (yellow). Boxes containing 10 asphaltene molecules, 300 solvent molecules (200 toluene molecules and 100 *n*-heptane molecules in the case of b), and 20 cardanol molecules or 6 addition polycardanol molecules or 3 condensation polycardanol molecules.

aggregates. Both cardanol and addition polycardanol seem to contribute to reduce the occurrence of the largest aggregates with six or more molecules. In the solvent mixture, additives seem to promote the formation of asphaltene dimers and prevent aggregates with 3 or more molecules, in particular, addition polycardanol. However, in toluene, all additives seem to promote the formation of small aggregates with less than seven molecules. In brief, all additives seem to have a dispersing effect in *n*-heptane and *n*-heptane/toluene mixtures but to promote the formation of small aggregates in toluene. The comparison between the three different additives is not easy because their performance depends on the solvent composition. Nevertheless, condensation polycardanol seems to be the most effective in reducing asphaltene precipitation, especially reducing the largest aggregates. Addition polycardanol seems more effective than cardanol in *n*-heptane, while the opposite is observed in the *n*-heptane/toluene solvent mixture.

In agreement with the present simulations, the experimental results of Lucas et al.^{42–45} have shown the asphaltene dispersion ability of cardanol and the flocculating effect of addition polycardanol in toluene. Moreover, experiments revealed a more efficient dispersion effect of addition polycardanol than the monomer, while the action of condensation polycardanol usually depends on the type and source of the asphaltene studied.

In Figure 12, radial distribution functions (rdf) between asphaltene CSA carbon atoms are shown for asphaltene in pure *n*-heptane, pure toluene, and in toluene/*n*-heptane mixtures with and without additives. In pure *n*-heptane, the

presence of cardanol and addition polycardanol seems to lower the first two peaks, which means a lower probability of asphaltene CSA–CSA interactions. This correlates with the trends previously described for these additives, namely, reducing the lifetime of asphaltene dimers and the number of larger aggregates. On the other hand, condensation polycardanol seems to produce a slightly different effect on the system: it considerably reduces the intensity of the rdf (which becomes a shoulder) but induces a new intense peak at a longer distance. Therefore, condensation polycardanol seems to contribute to change the preferential orientation between asphaltene molecules, probably favoring the *T*-shape orientation relatively to the parallel. This is also consistent with the tendency seen above to favor the formation of aggregates of intermediate size.

In the *n*-heptane/toluene mixture, a different picture is observed. The first two peaks of the rdf are clearly reduced by the presence of cardanol, but remain unchanged with addition polycardanol. In the case of condensation polycardanol, the first peak remains unchanged, but the second peak disappears, implying the absence of second shell neighbors. This correlates with the observation that, in the presence of condensation polycardanol, asphaltene molecules practically do not form aggregates with more than 4 molecules.

Finally, in toluene, the probability of asphaltene CSA–CSA interactions is higher in the presence of all additives, in particular, addition polycardanol. This is an expected result since, as previously described, in this solvent, the formation of dimers is promoted by all studied additives.

Table 4. Average Number of Hydrogen Bonds (HB) between Hydrogen (HOC) and Oxygen (OHC) of the Hydroxyl Group from Cardanol or Each Polycardanol and between the Same Hydrogen and Nitrogen Atom from Asphaltene (NAA), Along with the Ratio between the Two Types of Hydrogen Bond in Asphaltene Solutions in Pure Toluene, Pure *n*-Heptane, and the Toluene/*n*-Heptane Mixture, Using an Additive

	cardanol	polycardanol by addition	polycardanol by condensation
		<i>n</i> -Heptane	
number of HB (HOC–OHC)	9.6	7.9	17.9
number of HB (HOC–NAA)	7.0	6.9	1.9
HOC–NAA/HOC–OHC ratio	0.73	0.87	0.11
		<i>n</i> -Heptane + Toluene	
number of HB (HOC–OHC)	4.7	4.1	18.1
Number of HB (HOC–NAA)	4.0	4.1	1.2
HOC–NAA/HOC–OHC ratio	0.84	1	0.066
		Toluene	
number of HB (HOC–OHC)	3.7	3.8	13.7
number of HB (HOC–NAA)	2.4	3.5	0.88
HOC–NAA/HOC–OHC ratio	0.64	0.94	0.064

The asphaltene model molecule used in this work contains only one polar heteroatom, a “pyridinic” nitrogen atom whose ability to form hydrogen bonds in toluene or *n*-heptane as solvents is almost null. One of the possible interaction mechanisms between asphaltenes and the type of additives studied is the formation of hydrogen bonds between the heteroatom of asphaltene and the hydroxyl group of cardanol, both monomers and polymers. The number of hydrogen bonds between the asphaltene nitrogen atom and the hydrogen atom of OH groups from cardanol and polycardanol were calculated (integrating the corresponding rdfs) and are presented in Table 4. The number of hydrogen bonds between hydroxyl groups of cardanols or polycardanols was also calculated. As can be seen, the results show the existence of hydrogen bonds, both between hydroxyl groups of cardanol units (in the case of polycardanol, both inter and intramolecular) and between the nitrogen atom of asphaltene (NAA) and the OH group of cardanol. In almost all cases, the former are more important than the latter. It can also be seen that the ratio between the number of cross hydrogen bonds (H from cardanol with N from asphaltene) to hydrogen bonds between cardanols reaches its highest values for addition polycardanol, followed by cardanol, while condensation polycardanol presents the lowest values. In this latter case, the number of hydrogen bonds is particularly high, mostly of the HOC–OHC type and the intramolecular type.

On the other hand, it is also apparent that as the fraction of *n*-heptane increases, the number of hydrogen bonds of both kinds increases. It seems that the action of cardanol and addition polycardanol as dispersant additives is based on the interaction with asphaltenes by hydrogen bonds. For condensation polycardanol, this is not so apparent, as the total number of cross hydrogen bonds is quite low in all of the solvents. This can be caused by steric hindrance in the vicinity of hydroxyl groups of condensation polycardanol (Figure 13). The “tree” structure of condensation polycardanol can promote the aggregation of asphaltene molecules in small clusters, while the exposed alkyl chains can serve to interact with the aliphatic solvent preventing the formation of higher aggregates.

Figure 14 shows the spatial distribution functions of cardanol and both polycardanols around asphaltene. In the case of cardanol and addition polycardanol, the average close proximity and orientation between the asphaltene nitrogen and

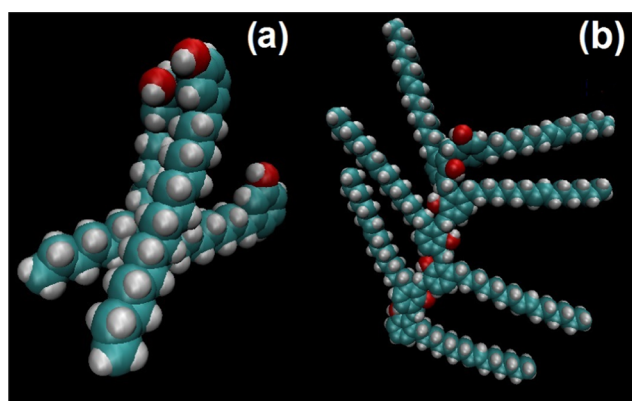


Figure 13. Representations (van der Waals radii) of (a) polycardanol by addition, (b) polycardanol by condensation.

the OH group of the additive is clear from the figure, most likely establishing hydrogen bonds. In the case of condensation polycardanol, the proximity between these groups is much less visible, probably due to the steric hindrance of condensation polycardanol.

4. CONCLUSIONS

Preaggregation phenomena of asphaltene in *n*-heptane, toluene, and *n*-heptane/toluene mixtures were studied by molecular dynamics simulation. The influence of dispersion additives such as cardanol, addition polycardanol, and condensation polycardanol was also investigated. The simulation results, namely, the frequency of asphaltene dimer formation, their lifetime, and the distribution of aggregates in the three solvents follow the trends observed in experimental work: a higher frequency of dimer formation and with a longer lifetime, as well as a higher probability of larger aggregates in *n*-heptane than in toluene. In *n*-heptane/toluene mixtures, the behavior of asphaltenes is intermediate, although closer to pure *n*-heptane.

The simulation results also revealed that all studied additives have a dispersion action in *n*-heptane and in *n*-heptane/toluene mixtures. In toluene, the additives, in particular, polymeric cardanols, seem to favor the formation of asphaltene dimers. The dispersion action of addition polycardanol and cardanol are comparable in magnitude. In the case of condensation polycardanol, it seems to promote small aggregates, preventing

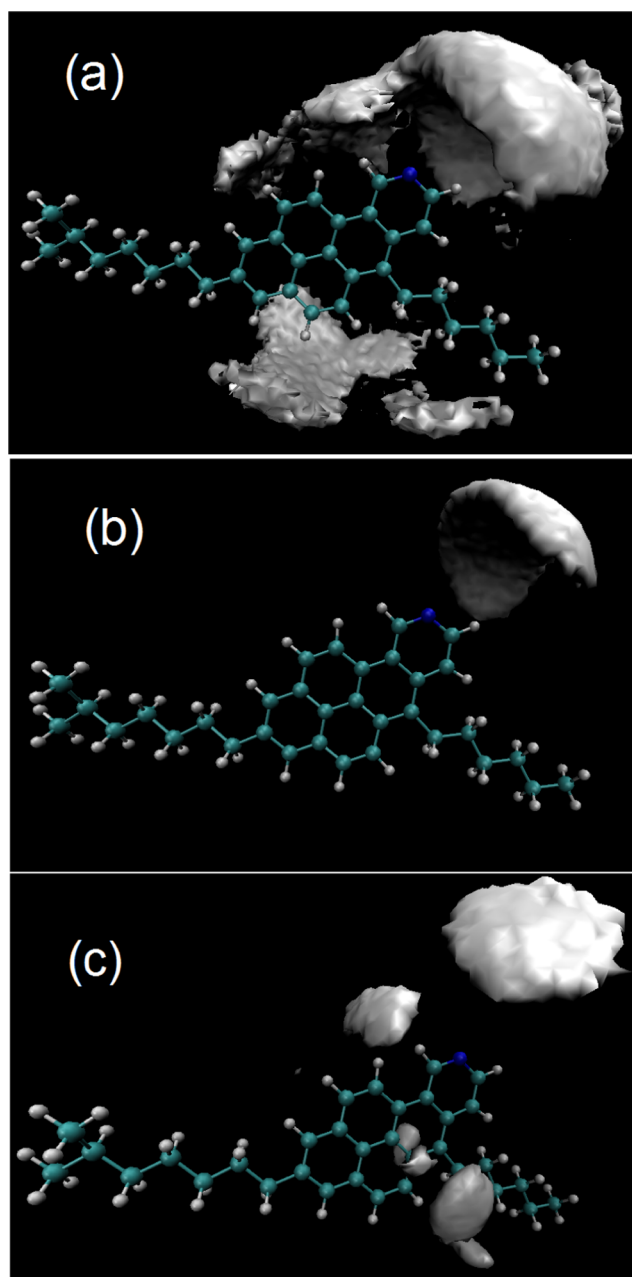


Figure 14. Spatial distribution functions of (a) cardanol (C1C atom), (b) addition polycardanol (C1P atom), and (c) condensation polycardanol (C1P atom) around asphaltene showing the isodensity surfaces with isovalues of 1.0 nm^{-3} .

large ones. Radial distribution functions between the central atoms of the asphaltene aromatic core confirmed the trends observed as a function of solvent composition and additive nature, since it is possible to correlate the intensity of the first peaks with the probability of asphaltene dimerization or the occurrence of larger asphaltene aggregates.

Hydrogen bonds seem to be the fundamental interaction between asphaltene and both cardanol and addition polycardanol, explaining the dispersion action of these additives. Condensation polycardanol, owing to high steric hindrance, has a very low tendency to form hydrogen bonds with asphaltene molecules.

AUTHOR INFORMATION

Corresponding Authors

Luís F. G. Martins – Centro de Química Estrutural, Instituto Superior Técnico, Universidade de Lisboa, Lisboa 1049-001, Portugal; Phone: +351 266 745 343; Email: lfgm@uevora.pt

Eduardo J. M. Filipe – Centro de Química Estrutural, Instituto Superior Técnico, Universidade de Lisboa, Lisboa 1049-001, Portugal; orcid.org/0000-0003-4440-7710; Phone: +351 218419261; Email: efilipe@tecnico.ulisboa.pt

Authors

Lucas G. Celia-Silva – Centro de Química Estrutural, Instituto Superior Técnico, Universidade de Lisboa, Lisboa 1049-001, Portugal

Patrícia B. Vilela – Centro de Química Estrutural, Instituto Superior Técnico, Universidade de Lisboa, Lisboa 1049-001, Portugal

Pedro Morgado – Centro de Química Estrutural, Instituto Superior Técnico, Universidade de Lisboa, Lisboa 1049-001, Portugal

Elizabete F. Lucas – Universidade Federal do Rio de Janeiro, IMA e COPPE, Rio de Janeiro 21941-594, Brazil; orcid.org/0000-0002-9454-9517

Complete contact information is available at:
<https://pubs.acs.org/10.1021/acs.energyfuels.9b03703>

Notes

The authors declare no competing financial interest.

ACKNOWLEDGMENTS

L.F.G.M. and L.G.C.S. acknowledge technical facilities from Instituto de Ciências da Terra (Evora University unit) and funding from FCT through the grant UID/QUI/0619/2019. P.B.V., P.M., and E.J.M.F. acknowledge funding from FCT through the project UID/QUI/0100/2013. We thank Professor João A. P. Coutinho for useful discussions.

REFERENCES

- (1) *Asphaltenes, Heavy Oils and Petroleomics*; Mullins, O. C.; Sheu, E. Y.; Hammani, A.; Marchall, A. G., Eds.; Springer: NY, 2007.
- (2) *Heavy Oils: Reservoir Characterization and Production Monitoring*; Chopra, S.; Lines, L. R.; Schmidt, D. R.; Batzle, M. L., Eds.; SEG Books: Tulsa, 2010.
- (3) Wiehe, I. A.; Liang, K. S. *Fluid Phase Equilib.* **1996**, *117*, 201–210.
- (4) Zhang, L.; Greenfield, M. L. *Energy Fuels* **2007**, *21*, 1102–1111.
- (5) Subramanian, S.; Simon, S.; Sjöblom, J. *J. Disp. Sci. Technol.* **2016**, *37*, 1027–1049.
- (6) Speight, J. G. *The Chemistry and Technology of Petroleum*, 4th ed.; CRC Press: Boca Raton, 2006.
- (7) Alvarez-Ramírez, F.; Ruiz-Morales, Y. *Energy Fuels* **2013**, *27*, 1791–1808.
- (8) Groenzin, H.; Mullins, O. C. *Energy Fuels* **2000**, *14*, 677–684.
- (9) Zhao, S.; Kotlyar, L. S.; Sparks, B. D.; Woods, J. R.; Gao, J.; Chung, K. H. *Fuel* **2001**, *80*, 1907–1914.
- (10) Murgich, J.; Abanero, J. A.; Strausz, O. P. *Energy Fuels* **1999**, *13*, 278–286.
- (11) Sheremata, J. M.; Gray, M. R.; Dettman, H. D.; McCaffrey, W. C. *Energy Fuels* **2004**, *18*, 1377–1384.
- (12) Headen, T. F.; Boek, E. S.; Jackson, G.; Totton, T. S.; Müller, E. A. *Energy Fuels* **2017**, *31*, 1108–1125.
- (13) Alshareef, A. H.; Scherer, A.; Tan, X.; Azyat, K.; Stryker, J. M.; Tykwinski, R. R.; Gray, M. R. *Energy Fuels* **2012**, *26*, 1828–1843.
- (14) Mullins, O. C. *Annu. Rev. Anal. Chem.* **2011**, *4*, 393–418.
- (15) Mullins, O. C. *Energy Fuels* **2010**, *24*, 2179–2207.

- (16) Mullins, O. C.; Sabbah, H.; Eyssautier, J.; Pomerantz, A. E.; Barré, L.; Andrews, A. B.; Ruiz-Morales, Y.; Mostowfi, F.; McFarlane, R.; Goual, L.; Lepkowitz, R.; Cooper, T.; Orbulescu, J.; Leblanc, J. M.; Edwards, J.; Zare, R. N. *Energy Fuels* **2012**, *26*, 3986–4003.
- (17) Goual, L.; Sedghi, M.; Mostowfi, F.; McFarlane, R.; Pomerantz, A. E.; Saraji, S.; Oliver, C.; Mullins, O. C. *Energy Fuels* **2014**, *28*, 5002–5013.
- (18) Mullins, O. C.; Seifert, D. J.; Zuo, J. Y.; Zeybek, M. *Energy Fuels* **2013**, *27*, 1752–1761.
- (19) Sedghi, M.; Goual, L.; Welch, W.; Kubelka, J. J. *Phys. Chem. B* **2013**, *117*, 5765–5776.
- (20) Silva, E. B.; Santos, D.; Alves, D. R. M.; Barbosa, M. S.; Guimarães, R. C. L.; Ferreira, B. M. S.; Guarnieri, R. A.; Franceschi, E.; Dariva, C.; Alexandre, F.; Santos, A. F.; Fortuny, M. *Energy Fuels* **2013**, *27*, 6311–6315.
- (21) Lesueur, D. *Adv. Colloid Interface Sci.* **2009**, *145*, 42–82.
- (22) Speight, J. G. *Oil Gas Sci. Technol.* **2004**, *59*, 467–477.
- (23) Lian, H.; Lin, J.-R.; Yen, T. F. *Fuel* **1994**, *73*, 423–428.
- (24) Marques, L. C. C.; Pereira, J. O.; Bueno, A. D.; Marques, V. A.; Lucas, E. F.; Mansur, C. R. E.; André, L. C.; Machado, González G. J. *Braz. Chem. Soc.* **2012**, *23*, 1880–1888.
- (25) Wiehe, I. A. *Energy Fuels* **2012**, *26*, 4004–4016.
- (26) Boukherissa, M.; Mutelet, F.; Modarressi, A.; Dicko, A.; Dafri, D.; Rogalski, M. *Energy Fuels* **2009**, *23*, 2557–2564.
- (27) Mutelet, F.; Ekulu, G.; Rogalski, M. J. *Chromatogr., A* **2002**, *969*, 207–213.
- (28) Mutelet, F.; Ekulu, G.; Solimando, R.; Rogalski, M. *Energy Fuels* **2004**, *18*, No. 667.
- (29) Chang, C. L.; Fogler, H. S. *Langmuir* **1994**, *10*, No. 1749.
- (30) Chang, C. L.; Fogler, H. S. *Langmuir* **1994**, *10*, No. 1758.
- (31) Goual, L.; Sedghi, M.; Wang, X.; Zhu, Z. *Langmuir* **2014**, *30*, 5394–5403.
- (32) Goual, L.; Sedghi, M. J. *Colloid Interface Sci.* **2015**, *440*, 23–31.
- (33) Hu, Y.-F.; Guo, T.-M. *Langmuir* **2005**, *21*, 8168–8174.
- (34) Fang, T.; Wang, M.; Li, J.; Liu, B.; Shen, Y.; Yan, Y.; Zhang, J. *Ind. Eng. Chem. Res.* **2018**, *57*, 1071–1077.
- (35) Murgich, J.; Rodríguez, M. J.; Aray, Y. *Energy Fuels* **1996**, *10*, 68–76.
- (36) Pacheco-Sánchez, J. H.; Zaragoza, I. P.; Martínez-Magadán, J. M. *Energy Fuels* **2003**, *17*, 1346–1355.
- (37) Pacheco-Sánchez, J. H.; Álvarez-Ramírez, F.; Martínez-Magadán, J. M. *Energy Fuels* **2004**, *18*, 1676–1686.
- (38) Carauta, A. N. M.; Seidl, P. R.; Chrisman, E. C. A. N.; Correia, J. C. G.; Menechini, P. O.; Silva, D. M.; Leal, K. Z.; de Menezes, S. M. C.; de Souza, W. F.; Teixeira, M. A. G. *Energy Fuels* **2005**, *19*, 1245–1251.
- (39) Headen, T. F.; Boek, E. S. *Energy Fuels* **2011**, *25*, 503–508.
- (40) AlHammadi, A. A.; Vargas, F. M.; Chapman, W. G. *Energy Fuels* **2015**, *29*, 2864–2875.
- (41) Abutaqiya, M. I. L.; Sisco, C. J.; Wang, J.; Vargas, F. M. *Energy Fuels* **2019**, *33*, 3632–3644.
- (42) Moreira, L. F. B.; Lucas, E. F.; González, G. J. *Appl. Polym. Sci.* **1999**, *73*, 29–34.
- (43) Mazzeo, C. P. P.; Stedille, F. A.; Mansur, C. R. E.; Ramos, A. C. S.; Lucas, E. F. *Energy Fuels* **2018**, *32*, 1087–1095.
- (44) Ferreira, S. R.; Louzada, H. F.; Dip, R. M. M.; González, G.; Lucas, E. F. *Energy Fuels* **2015**, *29*, 7213–7220.
- (45) Loureiro, T.; Dip, R. M.; Lucas, E. F.; Spinelli, L. *Journal of Polymers and the Environment* **2018**, *26*, 555–566.
- (46) Atta, A. M.; Abdullah, M. M. S.; Al-Lohedan, H. A.; Gaffer, A. K. *Energy Fuels* **2018**, *32*, 4873–4884.
- (47) Jorgensen, W. L.; Maxwell, D. S.; Tirado-Rives, J. J. *Am. Chem. Soc.* **1996**, *118*, 11225–11236.
- (48) Udier-Blagović, M.; Tirado, P. M.; Pearlman, S. A.; Jorgensen, W. L. *J. Comput. Chem.* **2004**, *25*, 1322–1332.
- (49) Ferreira, S. R.; Barreira, F. R.; Spinelli, L. S.; Leal, K. Z.; Seidl, P.; Lucas, E. F. *Química Nova* **2015**, *39*, 26–31.
- (50) Caleman, C.; van Maaren, P. J.; Hong, M.; Hub, J. S.; Costa, L. T.; van der Spoel, D. *J. Chem. Theory Comput.* **2012**, *8*, No. 2012.
- (51) Kashiwagi, H.; Hashimoto, T.; Tanaka, Y.; Kubota, H.; Makita, T. *Int. J. Thermophys.* **1982**, *3*, 201–215.
- (52) Harris, K. R.; Alexander, J. J.; Goscinska, T.; Malhotra, R.; L. A. Woolf, L. A.; Dymond, J. H. *Mol. Phys.* **1993**, *78*, 235–248.
- (53) Sagdeev, D. I.; Fomina, M. G.; Mukhamedzhanov, G. K.; Abdulagatov, I. M. *Int. J. Thermophys.* **2013**, *34*, 1–13.
- (54) Dullien, F. A. L. *AIChE J.* **1972**, *18*, 72–70.
- (55) Ryckaert, J. P.; Ciccotti, G.; Berendsen, H. J. C. *J. Comput. Phys.* **1977**, *23*, 327–341.
- (56) Smith, W.; Forester, T.; Todorov, I. *The DL_POLY Classic User Manual*; Daresbury Laboratory, 2012.
- (57) Van Der Spoel, D.; Lindahl, E.; Hess, B.; Groenhof, G.; Mark, A. E.; Berendsen, H. J. C. *GROMACS: Fast, Flexible and Free. J. Comput. Chem.* **2005**, *26*, 1701–1718.
- (58) Pronk, S.; Páll, S.; Schulz, R.; Larsson, P.; Bjelkmar, P.; Apostolov, R.; Shirts, M. R.; Smith, J. C.; Kasson, P. M.; van der Spoel, D.; Hess, B.; Lindahl, E. *GROMACS 4.5: a High-Throughput and Highly Parallel Open Source Molecular Simulation Toolkit. Bioinformatics* **2013**, *29*, 845–854.
- (59) Nosé, S. *Mol. Phys.* **1984**, *52*, 255–268.
- (60) Hoover, W. G. *Phys. Rev. A* **1985**, *31*, 1695–1697.
- (61) Toukmaji, A. Y.; Board, J. A., Jr. *Comput. Phys. Commun.* **1996**, *95*, 73–92.
- (62) Humphrey, W.; Dalke, A.; Schulten, K. *Journal of Molecular Graphics* **1996**, *14*, 33–38.
- (63) Brehm, M.; Kirchner, B. *J. Chem. Inf. Model.* **2011**, *51*, 2007–2023.
- (64) Bernardes, C. E. S.; Minas da Piedade, M. E.; Canongia Lopes, J. N. J. *Phys. Chem. B* **2011**, *115*, 2067–2074.
- (65) Bernardes, C. E. S. *J. Comput. Chem.* **2017**, *38*, 753–765.